AMERICAN SOCIETY FOR MICROBIOLOGY | Antimicrobial Agents and Chemotherapy

DNA Targeting as a Likely Mechanism Underlying the Antibacterial Activity of Synthetic Bis-Indole Antibiotics

Timothy J. Opperman,[a] Steven M. Kwasny,[a] Jessica Bo Li,[b] Mark A. Lewis,[b] Daniel Aiello,[a] John D. Williams,[a] Norton P. Peet,[a] Donald T. Moir,[a] Terry L. Bowlin,[a] Eric C. Long[b]

Microbiotix, Inc., Worcester, Massachusetts, USA[a]; Department of Chemistry and Chemical Biology, Indiana University-Purdue University Indianapolis, Indianapolis, Indiana, USA[b]

We previously reported the synthesis and biological activity of a series of cationic bis-indoles with potent, broad-spectrum antibacterial properties. Here, we describe mechanism of action studies to test the hypothesis that these compounds bind to DNA and that this target plays an important role in their antibacterial outcome. The results reported here indicate that the bis-indoles bind selectively to DNA at A/T-rich sites, which is correlated with the inhibition of DNA and RNA synthesis in representative Gram-positive (*Staphylococcus aureus*) and Gram-negative (*Escherichia coli*) organisms. Further, exposure of *E. coli* and *S. aureus* to representative bis-indoles resulted in induction of the DNA damage-inducible SOS response. In addition, the bis-indoles were found to be potent inhibitors of cell wall biosynthesis; however, they do not induce the cell wall stress stimulon in *S. aureus*, suggesting that this pathway is inhibited by an indirect mechanism. In light of these findings, the most likely basis for the observed activities of these compounds is their ability to bind to the minor groove of DNA, resulting in the inhibition of DNA and RNA synthesis and other secondary effects.

New therapeutic agents to treat infections caused by multidrug-resistant (MDR) pathogens represent a critical unmet medical need (1, 2). Toward this end, we recently reported a series of synthetic bis-indole agents (Fig. 1) that exhibit potent antibacterial activity *in vitro* against a broad spectrum of Gram-positive and Gram-negative pathogens (3–5). The most potent member of this series, MBX-1162 (Fig. 1), was found to be active (MIC_{90} values are reported in μg/ml) against methicillin-resistant *Staphylococcus aureus* (0.06 μg/ml) and *S. epidermidis* (0.015 μg/ml), vancomycin-resistant *Enterococcus faecalis* (0.015 μg/ml) and *E. faecium* (0.004 μg/ml), *Escherichia coli* (0.25 μg/ml), *Klebsiella pneumoniae* (0.5 μg/ml), *Proteus mirabilis* (2 μg/ml), *Pseudomonas aeruginosa* (1 μg/ml) (3), *Acinetobacter baumannii* (2 μg/ml) (5), and multidrug-resistant *Mycobacterium tuberculosis* (≤0.05 μg/ml) (6). Further testing also revealed that the bis-indoles are active in murine models of infection, increasing significantly the survival of mice that were infected with lethal doses of *Bacillus anthracis*, *S. aureus*, or *Yersinia pestis* (4). The bis-indoles exhibit rapid bactericidal activity against all organisms that have been tested to date: the viability of cultures of *B. anthracis*, *B. subtilis*, and *Y. pestis* were reduced by 10,000-fold in less than 4 h after treatment with MBX-1066 at 4× the known MIC (4). In addition, the bis-indoles exhibit potent antifungal activity against *Candida albicans*, *C. krusei*, *C. glabrata*, *C. parapsilosis*, and *Cryptococcus neoformans* and exhibit rapid fungicidal activity against *C. albicans* (7).

Given the potent antimicrobial activity of the bis-indoles, understanding the mechanism(s) of action that leads to the rapid bactericidal activity of these compounds is of interest. Preliminary mechanistic studies suggested that MBX-1066 selectively inhibits DNA synthesis in *B. subtilis* (4). In parallel work, several attempts to isolate mutants of *S. aureus* with reduced susceptibility to MBX-1066 (4) and MBX-1162 (unpublished data) were unsuccessful, suggesting that the bis-indoles do not inhibit a distinct protein or RNA target. Together, these observations raise the possibility that the bis-indoles act through a general, nonspecific mechanism. While the most likely nonspecific mechanism is disruption of the membrane potential or integrity, our studies indicated that the bis-indoles do not affect the transmembrane proton gradient or membrane integrity of *B. subtilis*, suggesting that some other fundamental target is probably involved (4). In a recent report, we have shown that the bis-indoles localize to the nucleus of the fungal pathogen *C. albicans* and strongly inhibit DNA synthesis (7), indicating that the potent antifungal activity of these compounds is likely to be the result of their DNA binding activity. This finding strongly suggests that the nonspecific target of the bis-indoles is DNA. Indeed, the bis-indole compounds studied here share several important structural and chemical features with well-established DNA minor groove-targeted compounds, such as DAPI (4′,6′-diamidino-2-phenylindole) (Fig. 1). These features include "sickle-shaped," planar structures, terminally positioned cationic functionalities, and heteroatoms with the potential to form hydrogen bonds with the floor of the minor groove of B-form DNA.

To investigate the antibacterial mechanism of the bis-indoles, we carried out studies to test the hypothesis that DNA binding activity of these compounds plays an important role in their antibacterial activity. Here, we report the results of studies that verified DNA binding in cells, determined the composition of DNA

Received 5 February 2016 **Returned for modification** 5 March 2016
Accepted 4 September 2016

Accepted manuscript posted online 12 September 2016

Citation Opperman TJ, Kwasny SM, Li JB, Lewis MA, Aiello D, Williams JD, Peet NP, Moir DT, Bowlin TL, Long EC. 2016. DNA targeting as a likely mechanism underlying the antibacterial activity of synthetic bis-indole antibiotics. Antimicrob Agents Chemother 60:7067–7076. doi:10.1128/AAC.00309-16.

Address correspondence to Timothy J. Opperman, topperman@microbiotix.com, or Eric C. Long, eclong@iupui.edu.

Supplemental material for this article may be found at http://dx.doi.org/10.1128/AAC.00309-16.

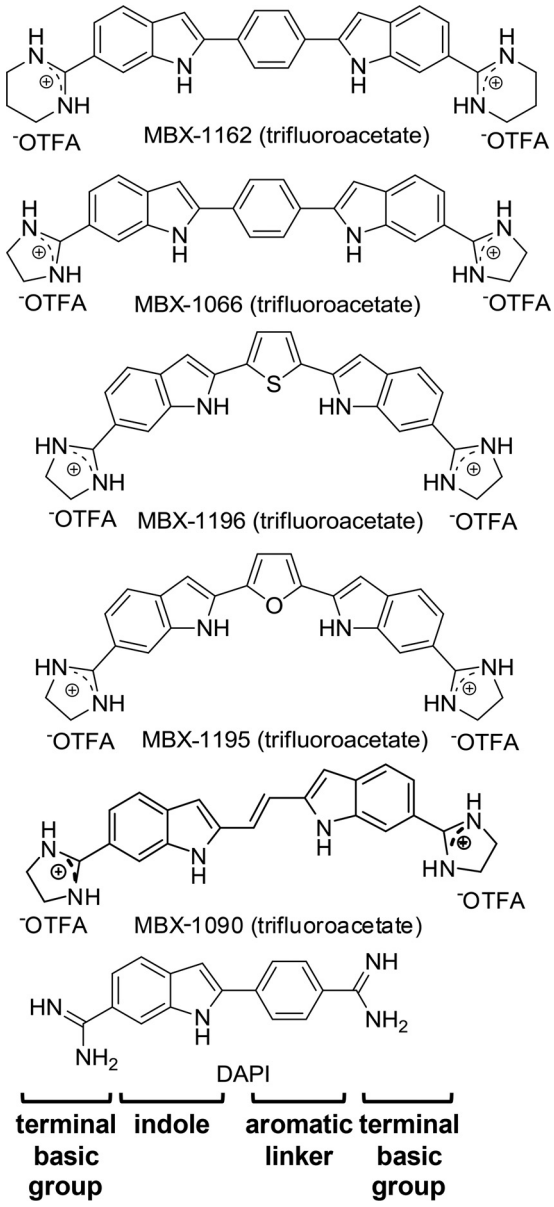

FIG 1 Chemical structures of the bis-indole compounds used in this study compared to the DNA minor groove binding dye DAPI.

sequences targeted selectively by the bis-indole compounds in this series, and evaluated their relative binding affinities to a preferred DNA sequence. In addition, we measured the biological consequences of DNA binding on macromolecular synthesis pathways and stress response. Taken together, the results of our experiments support the hypothesis that the primary cellular target of this series of bis-indoles is DNA. Further, these findings support a link between the DNA binding activity of these compounds and their cytotoxicity against mammalian cells, which limits their potential use as antimicrobial agents.

MATERIALS AND METHODS

Bacterial strains and growth conditions. The following bacterial strains were used in these studies: *Staphylococcus aureus* NCTC 8325 (8), *S. aureus* RN4220 (pAmi-Rec) (9), *S. aureus* RN4220 (pAmi-vraX) (this study [see below]), *Escherichia coli* KLE700 (WT) and KLE701 (Δ*tolC*) (10), GW1000 [F$^-$ *thr-1 araC14 leuB6* Δ(*argF-lac*)*169 tsx-33 glnV44 galK2* λ$^-$ *sulA211 hisG4 recA441*(ts) *rpsL31*(strR) *xylA5 argE3*(Oc) *thi-1 ilv*(ts)] (11), GW1000 *lexA3*(Ind−), GW1000 Δ*lexA300*::spec(Def), GW1000 Δ*recA*::kan, and GW1000 *glmS*::mini-Tn*7* (P_{sulA}-*luxCDABE*, FRT-gent-FRT). To construct the SOS reporter strain GW1000 *glmS*::mini-Tn*7* (P_{sulA}-*luxCDABE*, FRT-gent-FRT), the promoter of the SOS-regulated gene *sulA* was amplified using a PCR programmed with the primers P_{sulA}-Dra-L (ATCGCTCCCACTATGTGCGGATCCGTTAACTACGAAAA) and PsulA-Dra-R (CATCGCTCCCACCGCGTGGCCCCTGTGAGTTA CTGTATGG), which contain unique DraIII restriction sites (underlined) to enable directional cloning upstream of the *luxCDABE* operon *of Photorhabdus luminescens* (12), which is carried in the mini-Tn*7* element of pUC18R6K-mini-Tn*7*T-Gm (13). The resulting P_{sulA}-*luxCDABE* reporter construct was transferred to a unique site (*glmS*) in the chromosome of *E. coli* TOP10 as previously described (13) and was transferred to GW1000 using P1 transduction. The *S. aureus* reporter plasmid pAmi-vraX was constructed as follows. The promoter of the *vraX* gene in *S. aureus*, which is induced in response to cell wall stress (14–16), was amplified using PCR programmed with primers P_{vraX}-F (AATTTGGATCC TGATTTTGTTGGTCCTGTGG) and P_{vraX}-R (ATTAAGTCGACACCT CCTTTGCTACTCTATGGTT), which contain restriction sites for BamHI and SalI (underlined), respectively. The *vraX* promoter fragment was cloned into the BamHI and SalI sites of pAmi-lux (17) using standard methods, and the recombinant plasmid was transferred to *S. aureus* using electroporation. All strains were grown in tryptic soy broth (TSB) at 37°C on a platform shaker (250 rpm). Reserpine (20 μg/ml) was added to cultures of *S. aureus* to inhibit efflux pump activity (18).

Chemicals. The bis-indoles used in the present study (Fig. 1) were synthesized at Microbiotix, Inc., as described previously (19). Netropsin, ciprofloxacin, vancomycin, sanguinarine, and DAPI were purchased from Sigma-Aldrich (St. Louis, MO).

Visualization of bis-indoles in bacteria using fluorescence microscopy. An exponentially growing culture of *S. aureus* (OD_{600} ~ 0.4) was treated with MBX-1066 at concentrations equivalent to 0×, 1×, and 4× the MIC for 30 min at room temperature. A culture of *E. coli* KLE701 was grown in the presence of 10 μM sanguinarine (Sigma-Aldrich), which blocks cell division by inhibiting polymerization of FtsZ (20), resulting in filamented cells. The treated cells were fixed with 0.04% glutaraldehyde and 2.5% formaldehyde for 30 min and then stained with either MBX-1066 at 4× the MIC or 0.3 μM Syto 9 (Molecular Probes, Portland, OR) for 30 min. After staining, the cells of *S. aureus* and *E. coli* were harvested and resuspended in water containing 0.02% agarose, and a total of 5 μl of each suspension was placed on a microscope slide, covered with a coverslip, and visualized under light (differential interference contrast [DIC]) and fluorescence microscopy using the DAPI and fluorescein isothiocyanate filter sets to visualize MBX-1066 and Syto 9, respectively.

Analyses of DNA binding. The DNA binding site selectivity of each bis-indole compound was determined by using a fluorescence intercalator displacement (FID) assay (21–25). The 136-member hairpin deoxyoligonucleotide library required for this study contained binding sites of 4 bp and was purchased from Trilink Biotechnologies, Inc., as individual lyophilized solids. The concentrations of the hairpin oligodeoxynucleotides were determined as described previously (21) using UV at 90°C and single-strand extinction coefficients to ensure accurate concentration determination. All bis-indole compounds examined were initially prepared as 10 mM dimethyl sulfoxide (DMSO) stock solutions.

FID analyses were carried out using Costar black 96-well plates loaded with sodium cacodylate buffer containing ethidium bromide (EtBr; 150 μl of 6 μM EtBr, 120 mM NaCl, and 12 mM sodium cacodylate [pH 7.4]). To each well was added one hairpin oligodeoxynucleotide of the library (30 μl of 10 μM hairpin solution, which is equivalent to 70 μM in base pairs, dissolved in H_2O). The final concentrations in each well were 1.5 μM DNA-hairpin, 4.5 μM EtBr, and 0.75 to 2 μM DNA binding agent. The final buffer consisted of 10 mM sodium cacodylate (pH 7.4)–100 mM

NaCl. After incubation at 25°C for 30 min, each well was read on a Varian Cary Eclipse fluorescence plate reader (λ_{Ex}, 545 nm; λ_{Em}, 595 nm). Compound assessments were conducted with each well acting as its respective control well (no agent = 100% fluorescence; no DNA = 0% fluorescence). Fluorescence readings are reported as the percent fluorescence decrease relative to the control wells.

Titrations to determine relative binding affinities were carried out using a 50-μl quartz microcuvette loaded with sodium cacodylate buffer (containing 100 mM NaCl and 10 mM sodium cacodylate [pH 7.4]) and ethidium bromide (4.5 μM final concentration); the total volume was 50 μl. Sample fluorescence was measured on a Varian Cary Eclipse spectrofluorometer and normalized to 0% fluorescence. At this point, the hairpin deoxyoligonucleotide AATT was added to a concentration of 1.5 μM (hairpin final concentration), and the resulting fluorescence was normalized to 100%. Titrations were conducted by adding aliquots of agent (0.5 μl aliquots of 0.15 μM bis-indole in buffer) and measuring the resulting fluorescence decrease after a 5-min equilibration time. Compound additions were continued until the system reached saturation and the fluorescence remained constant with subsequent additions of agent. Data provided by these titrations were analyzed through standard Scatchard binding analyses exactly as described previously (21, 23).

Macromolecular synthesis assays. The effects of the bis-indoles and netropsin on various macromolecular synthetic pathways in *S. aureus* NRS-77 (NCTC 8325) and *E. coli* KLE701—DNA, RNA, protein, lipid, and peptidoglycan synthesis—were measured as described previously (26). Because the presence of active efflux pumps significantly decreases the antibacterial activity of MBX-1195, the effect of efflux on the activity of all the test compounds in the macromolecular synthesis (MMS) assay was minimized by using an efflux-defective strain of *E. coli* KLE701 [Δ*tolC*]) or by growing *S. aureus* in the presence of 20 μg of reserpine/ml, an efflux pump inhibitor. Briefly, bacterial cultures were grown aerobically in Luria-Bertani (LB) medium at 37°C to midlogarithmic growth phase (i.e., an optical density at 600 nm [OD_{600}] of 0.1 to 0.2). The cultures were added to prewarmed (37°C) 96-well assay plates that were loaded with 50 μl of LB media containing a radiolabeled precursor at twice the final concentration and test compounds at concentrations ranging from 0.16× to 16× the MIC. The radiolabeled precursors used for each macromolecular synthetic pathway were as follows: [^{3}H]thymidine (DNA), [^{3}H]uridine (RNA), [^{3}H]leucine (protein), [^{3}H]acetate (lipid), and [^{3}H]-*N*-acetylglucosamine (peptidoglycan). The final concentration of DMSO in each well, including the untreated controls, was 2%. The assay plates were incubated at 37°C for 20 min, which is less than the doubling time of *E. coli* and S. aureus (~40 min) under the conditions of the assay. To terminate the assay and to precipitate macromolecules, 100 μl of 20% trichloroacetic acid (TCA) was added to each well, and the assay plates were placed on ice for 30 min. The precipitated macromolecules were collected by filtration in 96-well MultiScreen (Millipore) filter plates with glass fiber filters. After repeated washes with 5% TCA and then 95% ethanol, the plates were dried, and the amount of radioactivity bound to each filter was measured with a Perkin-Elmer MicroBeta scintillation counter. Each compound was tested in triplicate on the same assay plate, each data point represents the average of three replicates, and the error bars represent the standard deviations. The concentration that inhibited each macromolecular synthetic pathway by 50% (IC_{50}) was determined using the four-parameter nonlinear curve-fitting function of GraphPad Prism (GraphPad Software). To monitor assay specificity, the following pathway-specific antibiotics were included in each assay: ciprofloxacin (DNA), rifampin (RNA), ampicillin (cell wall-*E. coli*), vancomycin (cell wall-S. *aureus*), irgasan (lipid), and chloramphenicol (protein).

Antibacterial activity assays. The MIC of antibacterial agents and biocides were determined using the broth microdilution method essentially as described in Clinical and Laboratory Standards Institute protocol M7-A7 (27), except that LB medium was used instead of Mueller-Hinton broth. Serial 2-fold dilutions of test compounds were made in DMSO at concentrations 50-fold higher than the final concentration: the diluted compounds were added to the assay plates, and 100 μl of the inocula was added to each well. The final concentration of DMSO in each assay was 2%. To determine the effect of serum on the antibacterial activity of the bis-indoles, 10% fetal bovine serum (FBS; Gibco) was added to the growth medium at a final concentration of 10%.

Killing curve assays were performed essentially as described previously (28). Exponential bacterial cultures grown in LB medium were diluted to a cell density of ~10^7 in LB medium, followed by the addition of MBX-1162 to a minimally bactericidal concentration (0.06 μg/ml). Viability was monitored over 4 h by removing samples, making serial dilutions in saline, and spotting 5 μl of each dilution onto the surface of an LB agar plate in triplicate. Colonies were counted after the plates were incubated at 37°C for 16 to 18 h, the CFU per ml were calculated, and the averages and standard deviations for the three replicates were determined. Each experiment was repeated at least three times, and the results from a representative experiment are shown.

Cytotoxicity versus mammalian (HeLa) cells. The cytotoxicity of test compounds against HeLa cells (ATCC CCL-2) was determined as described previously (29). Briefly, each well of a 96-well plate was seeded with 4,000 cells of HeLa cells in 200 μl of minimum essential medium containing 1× Earle's salts, 1.5 g/liter sodium bicarbonate (GE Healthcare), and 10% FBS. After the cells attached (2 to 4 h), 2 μl of various concentrations (2-fold dilution series) of compounds dissolved in DMSO were added to the media, and the plates were incubated at 37°C in a 5% CO_2 atmosphere for 3 days. The cell viability in each well was measured using the redox sensitive dye MTT [3-(4,5-dimethylthiazol-2-yl)-2,5-diphenyltetrazolium bromide]. The absorbance of each well was plotted as a fraction of the untreated versus drug concentration, and the concentration that produces 50% cytotoxicity (CC_{50}) was determined using the four-parameter nonlinear curve-fitting function of GraphPad Prism (GraphPad Software).

Cell-based reporter assays. For SOS cell-based reporter assays, *E. coli* GW1000 *glmS*::mini-Tn*7* (P_{sulA}-*luxCDABE*, FRT-gent-FRT) or *S. aureus* RN4220 (pAmi-Rec) were grown to mid-log phase (OD_{600} ~ 0.2) in tryptic soy broth at 37°C, and 100 μl was transferred to each well of a 96-well microassay plate (Costar 3915) containing various amounts of a bis-indole or netropsin (0.125× to 4× the MIC). Ciprofloxacin (CIP) was used as a positive control at a concentration of 5× the MIC (0.1 μg/ml) for *E. coli* and 2× the MIC (2 μg/ml) for *S. aureus*. Each condition was replicated in a total of eight separate assay wells (one column on the assay plate). The assay plate was placed in a Victor3 V, and light emission was monitored over time at 37°C. The average values and standard deviations for the eight replicates were calculated. The fold induction for each treatment compared to the untreated control has been plotted as a function of time. The procedure described above was also used for the cell wall stress stimulon reporter assays, except that *S. aureus* RN4220 (pAmi-vraX) was used as the reporter strain and vancomycin at a concentration of 2× the MIC (4 μg/ml) was used as the positive control.

RESULTS AND DISCUSSION

Biological activities of the bis-indoles. The antibacterial activities (MIC) and mammalian cell cytotoxicities (CC_{50}) of the bis-indoles (see Fig. 1) used in this study are shown in Table 1. The bis-indoles exhibit potent antibacterial activity against *S. aureus* and *E. coli*. In addition, the bis-indoles are rapidly bactericidal against *S. aureus* and *E. coli*. As shown in Fig. 2, MBX-1162 (4× the MIC) reduced the numbers of viable cells by 5 logs within 2 h. The antibacterial activity of the bis-indoles was not affected by the presence of 10% FBS or efflux, with the exception of MBX-1195, which had no measureable activity against efflux proficient organisms. To compare directly the activities of the bis-indoles, we performed all assays using an efflux-defective strain of *E. coli* (KLE701 [Δ*tolC*]) or *S. aureus* treated with inhibitor of efflux (20 μg of reserpine/ml).

TABLE 1 Antibacterial activity and cytotoxicity values for various compounds[a]

Organism	Strain	Efflux[b]	% FBS	MIC (μg/ml)[c]						
				MBX-1066	MBX-1090	MBX-1162	MBX-1195	MBX-1196	CIP	NET
S. aureus	NRS-77	+	0	0.062	1	0.062	≥32	0.12	0.12	
		–	0	0.062	0.5	0.062	1	0.12	0.12	16
		–	10	0.062	0.5	0.062	1	0.12	0.062	
E. coli	KLE700	+	0	0.5	2	0.5	≥32	0.5	0.016	
	KLE701	–	0	0.25	0.5	0.25	4	0.5	0.002	16
	KLE701	–	10	0.25	0.5	0.25	2	0.25	0.002	
HeLa cells (CC_{50} [μg/ml])			10	32.5	10	4	15	15	ND	ND

[a] FBS, fetal bovine serum; CIP, ciprofloxacin; NET, netropsin; ND, not determined; CC_{50}, concentration that produces 50% cytotoxicity.
[b] +, efflux proficient; −, efflux deficient.
[c] Note that the bottom row of data show CC_{50} (μg/ml) values.

***In vitro* and *in situ* DNA binding assays.** The structural similarities shared by the bis-indoles and DAPI (Fig. 1), a well-established dye that fluoresces strongly when bound to the minor groove of A/T-rich double-stranded DNA (λ_{ex} = 358 nm; λ_{em} = 461 nm), suggest that the bis-indoles may target and bind to DNA. To test this possibility, the fluorescence of a representative bis-indole, MBX-1066, was examined in the presence or absence of *Bacillus anthracis* genomic dsDNA. Samples containing a fixed concentration of this DNA (4 μg/ml, equivalent to 3 μM bp) were combined with various amounts of MBX-1066 and monitored for changes in fluorescence intensity (λ_{ex} = 390 nm, λ_{em} = 460 nm). As shown in Fig. 3A, the fluorescence intensity of the sample increased steadily upon the addition of MBX-1066 up to 6 μM total MBX-1066 representing a 2:1 bis-indole/DNA base-pair ratio. The fluorescence decreases observed with additions of compound beyond the 2:1 point of charge neutralization were most likely due to precipitation of the DNA. In comparison, the fluorescence of samples containing MBX-1066 alone (no DNA) did not change over the same concentration range. These results clearly indicate that MBX-1066 binds to DNA *in vitro* and does so in a manner that results in increased bis-indole fluorescence. Taken together, the evidence indicates that the bis-indoles bind to DNA *in vitro*.

To verify that MBX-1066 can bind to DNA within intact bacterial cells, exponentially growing cultures of *S. aureus* NCTC 8325 were treated with 0.5 μg/ml MBX-1066 (4× the MIC) and viewed via light and fluorescence microscopy using a DAPI filter.

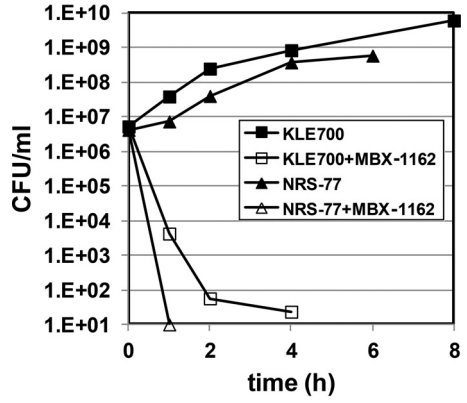

FIG 2 MBX-1162 is rapidly bactericidal against *E. coli* KLE700 and *S. aureus* NRS-77 at a concentration equivalent to 4× the MIC.

As shown in Fig. 3B, cells treated with MBX-1066 were fluorescent, but untreated cells were not, suggesting that MBX-1066 binds to the genomic DNA present in living cells of *S. aureus*. To confirm that the MBX-1066-derived fluorescence colocalized with bacterial genomic DNA, filamented *E. coli* cells were produced by growth in the presence of sanguinarine, treated with MBX-1066 or the DNA intercalating dye Syto9, and then examined using light and fluorescence microscopy. Sanguinarine treatment, as expected, resulted in filamentous cells with multiple, discrete nucleoids containing genomic DNA. As shown (Fig. 3C), the filaments contained discrete nucleoids that exhibited colocalized Syto9 and MBX-1066 fluorescence, verifying that MBX-1066 can target and bind genomic DNA in intact bacterial cells.

Examination of DNA binding sequence selectivity. The DNA binding activities of the bis-indoles were assessed in greater detail using a standard FID assay that can identify preferred sites of drug-DNA binding and their rank order (21–25). In brief, the FID assay measures the ability of a compound to displace a fluorescent DNA intercalating agent (ethidium bromide) that is bound to double-stranded DNA; binding competition results in decreased fluorescence. To identify the preferred binding sites of these compounds, we used the FID assay to screen libraries of synthetic hairpin oligonucleotides containing all possible 4- or 5-bp double-stranded DNA binding sites (136 or 512 individual DNA oligonucleotides, respectively). The relative fluorescence decreases for each oligonucleotide were rank ordered and displayed in the form of a histogram to visualize the DNA sequences of preferred binding and to compare the selectivity of DNA binding among this series of compounds. The histograms for MBX-1066 and MBX-1162 are shown in Fig. 4A and B, respectively. The histograms illustrate that both compounds bind preferentially to sequences composed exclusively of A/T base pairs and that MBX-1162 produced greater decreases in fluorescence than MBX-1066, indicating a higher DNA binding affinity. In comparison, MBX-1196 displayed an FID histogram profile that was qualitatively most similar to MBX-1162, while MBX-1195 was similar to MBX-1066; MBX-1090 displayed a profile that was intermediate between these two extremes (see Fig. S1 in the supplemental material).

Further examination of the top sequences selected by each of the bis-indoles identified the nucleotide compositions of preferred sequences to be 5′-AATT and 5′-AAAT. To assess the relative affinities of the bis-indoles for the preferred binding site

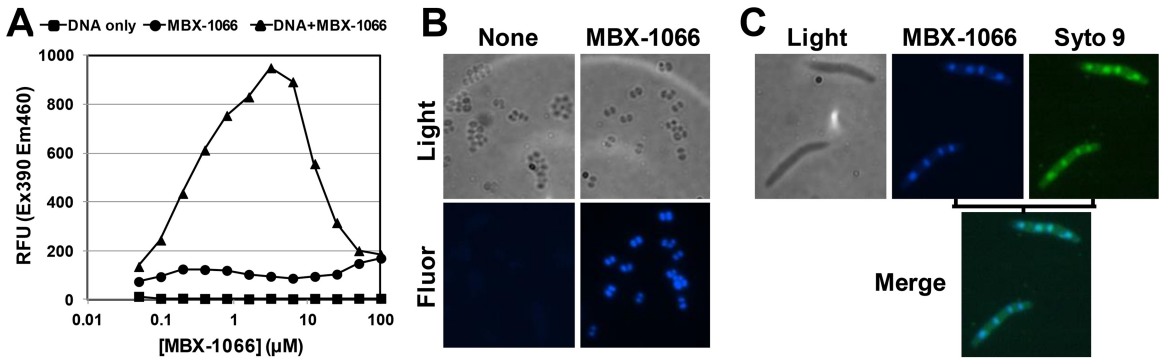

FIG 3 The increased fluorescence of MBX-1066 in the presence of DNA and in bacterial cells is consistent with DNA binding. (A) Fluorescence enhancement of MBX-1066 in the presence of genomic DNA. The fluorescence (RFU) of various concentrations of MBX-1066 in the presence of *Bacillus anthracis* genomic DNA (6 μM nucleotides) was measured as the emission at 460 nm after excitation with 390 nm. (B) MBX-1066 fluorescence in bacterial cells is consistent with selective DNA binding. Living cells of *S. aureus* NCTC 8325 were exposed to 0.5 μg of MBX-1066/ml and viewed under light and fluorescence microscopy using a DAPI filter. (C) MBX-1066 fluorescence is colocalized to nucleoids in fixed cells of *E. coli*. A culture of *E. coli* 701 (Δ*tolC*) was grown in the presence of the cell division inhibitor sanguinarine (10 μM). The cells were fixed and stained with MBX-1066 (1× the MIC) and the DNA intercalating dye Syto9 and viewed under light (DIC) and fluorescence microscopy using DAPI and green fluorescent protein filters to visualize MBX-1066 and Syto9, respectively.

AATT, quantitative titrations of each compound were tested in the FID assay, and the results were subjected to Scatchard analyses to estimate the binding affinity (K_a). The relative affinities of the bis-indoles for 5′-AATT were as follows: MBX-1162 ($K_a = 31 \times 10^6\ M^{-1}$) > MBX-1196 ($K_a = 1 \times 10^6\ M^{-1}$) > MBX-1066 ($K_a = 0.5 \times 10^6\ M^{-1}$) ≈ MBX-1090 ($K_a = 0.3 \times 10^6\ M^{-1}$) ≫ MBX-1195 ($K_a$ not determined, as it was too weak). These values indicated that the binding affinity of the most potent bis-indole (MBX-1162) to AATT is closest to that displayed by netropsin ($65 \times 10^6\ M^{-1}$) when measured by similar experimental means (21, 23); the remaining compounds are best classified as moderate or relatively weak DNA binding agents. Importantly, in common with many other A/T-targeted agents, the bis-indoles display a preference for AATT sites. Previous studies have shown that

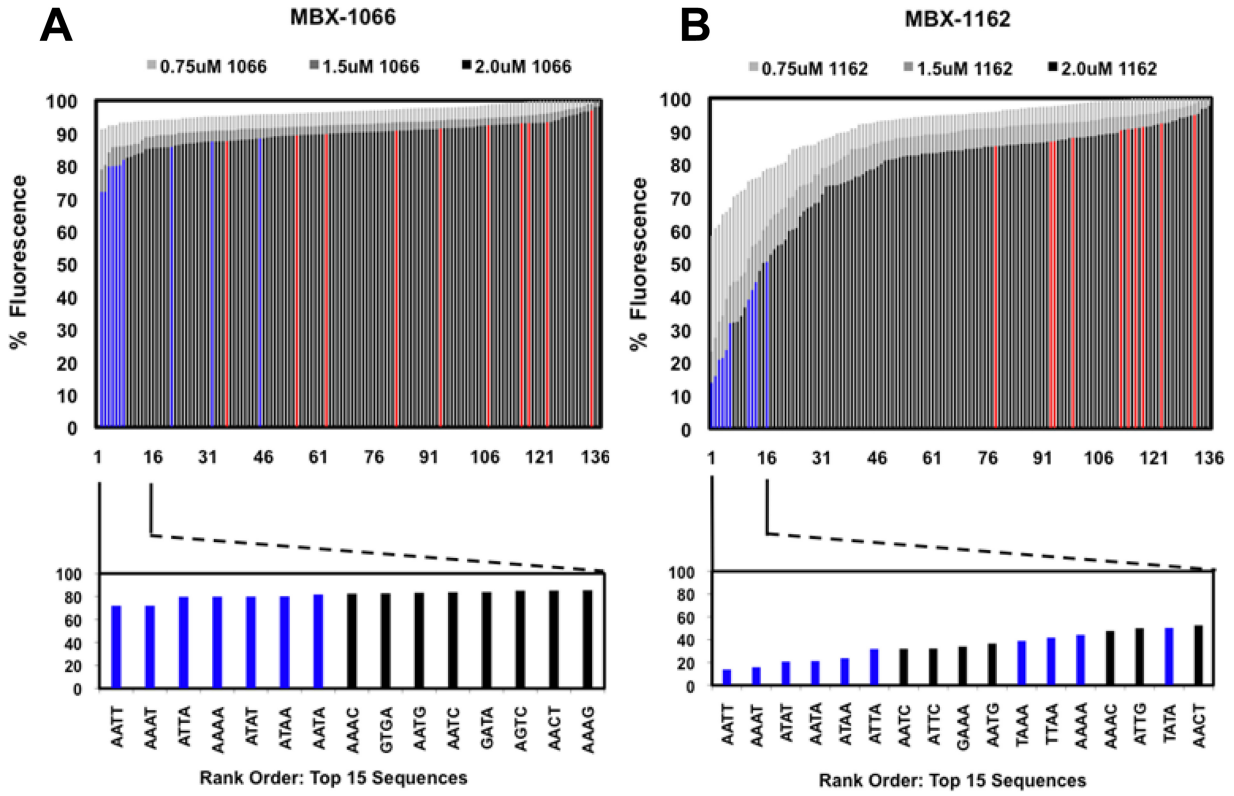

FIG 4 Merged-bar histograms resulting from FID analyses of compounds MBX-1066 (A) and MBX-1162 (B). Each compound was analyzed at 0.75, 1.5, and 2.0 μM concentrations; the results for the 2.0 μM analyses are color-coded as follows: red, G/C-only 4-bp oligonucleotide cassettes; blue, A/T-only 4-bp cassettes; and black, mixed sequence cassettes. The sequences of the top 15 rank-ordered oligonucleotides are shown in each plot expansion. The highest ranking binding sequence for both MBX-1066 and MBX-1162 was 5′-AATT.

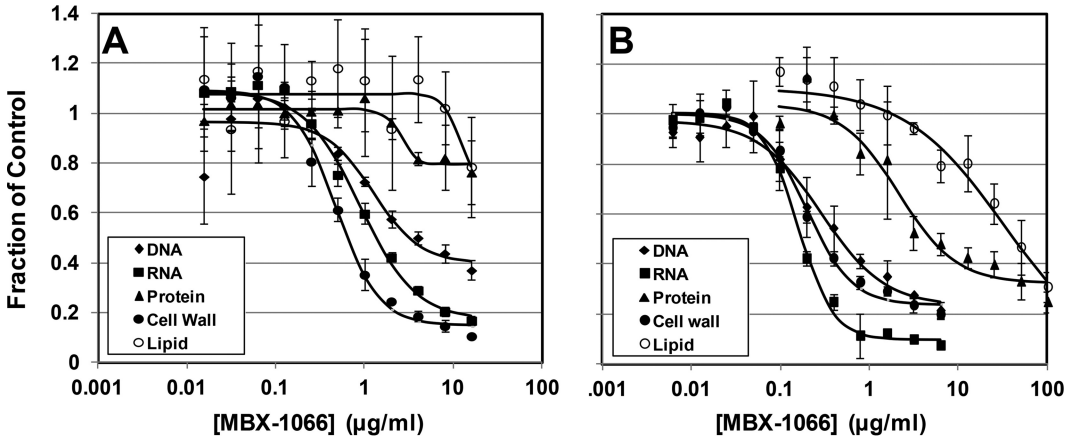

FIG 5 Representative MMS assays indicate bis-indoles primarily inhibit DNA, RNA, and cell wall biosynthesis in *S. aureus* and *E. coli*. (A) *E. coli* KLE701 treated with MBX-1066; (B) *S. aureus* NRS-77 treated with MBX-1066.

AATT sites are conducive to minor groove binding due to the characteristic width and depth of the minor groove (30, 31). Collectively, the observations described above support the notion that the MBX bis-indoles target the DNA minor groove and, like other synthetic minor groove binders (32–34), display a range of DNA binding affinities influenced by their structural differences (e.g., the nature of the central linker, the extent of the overall compound curvature, and substituent sizes).

Effects of DNA binding on MMS. To examine the effect of DNA binding on the physiology of bacterial cells, we measured the dose-dependent effects of MBX-1066, MBX-1162, and MBX-1195 on each of the major bacterial macromolecular synthetic (MMS) pathways in *E. coli* and *S. aureus*. The assay was terminated after 20 min of exposure, which is less than the doubling time of ~40 min for both organisms in the assay. The resulting dose-response curves were analyzed with a four-parameter curve-fitting algorithm to calculate the half-maximal inhibitory concentrations (IC_{50}s) for each compound against each of the MMS pathways, which provides a quantitative measurement for the inhibitory activities of a compound against each pathway. Netropsin, an antibacterial compound known to bind to the minor groove of DNA (35), was used as a control in the experiment. Representative dose-response curves are shown in Fig. 5, and the IC_{50}s of each compound for each of the MMS pathways in *E. coli* and *S. aureus* are shown in Table 2. In contrast to our previous results (4), which showed that MBX-1066 inhibits DNA synthesis in *B. subtilis*, the results from this more sensitive assay protocol show that the two bis-indoles that bind to DNA with a high affinity (MBX-1066 and MBX-1162) inhibited all of the MMS pathways in *S. aureus* and *E. coli* at relatively low concentrations but were most active against RNA, DNA, and cell wall synthesis. The control compound netropsin was most active against RNA synthesis in *S. aureus* and against DNA and RNA synthesis in *E. coli*. In contrast, MBX-1195 (undetectable affinity for DNA) inhibited RNA and cell wall synthesis in *S. aureus* and inhibited all pathways at relatively high concentrations in *E. coli* (Table 2). The results of these studies indicate that the effects of the DNA binding bis-indoles compounds on bacterial physiology is more complicated than was indicated by our previous results using *B. subtilis* alone (4), possibly due to differences between bacterial species, assay conditions, and efflux pump activity. We think that the current results accurately portray the mechanisms of action of the bis-indoles, since it is unlikely that the DNA binding activity of these compounds alone could account for their rapid bactericidal activity.

Despite the issues noted above, the current findings showing that MBX-1066 and MBX-1162 are most potent against DNA and RNA synthesis are consistent with the outcomes of studies of another series of DNA binding antibacterial agents (36). The potent inhibition of DNA and RNA synthesis observed in our studies is most likely to be the consequence of the DNA binding activity of

TABLE 2 Half-maximal inhibitory concentrations for bis-indoles and netropsin determined using macrcomolecular synthesis assays with *E. coli* and *S. aureus*

Organism	Treatment[a]	IC_{50} ± SD (μg/ml)				
		DNA	RNA	Protein	Cell wall	Lipid
S. aureus	MBX-1066	0.53 ± 0.14	0.18 ± 0.01	3.96 ± 0.97	0.29 ± 0.03	44.4 ± 16
NRS-77	MBX-1162	0.10 ± 0.02	0.06 ± 0.01	0.99 ± 0.42	0.09 ± 0.002	4.31 ± 1.1
NRS-77 + reserpine	MBX-1195	≥16	4.7 ± 2	≥16	9.8 ± 4.3	≥16
	NET	149.4 ± 31.4	48.6 ± 12.4	≥256	139.6 ± 38.2	≥256
E. coli KLE701 (Δ*tolC*)	MBX-1066	3.39 ± 0.5	1.37 ± 0.14	≥16	0.64 ± 0.06	≥16
	MBX-1162	0.12 ± 0.02	0.08 ± 0.002	0.25 ± 0.02	0.06 ± 0.006	0.85 ± 0.36
	MBX-1195	10.2 ± 3.8	14.1 ± 5.3	37.7 ± 10.4	21.6 ± 17.3	22.4 ± 9.7
	NET	53.5 ± 7.2	40.7 ± 4.7	≥256	≥256	120.5 ± 25.8

[a] NET, netropsin.

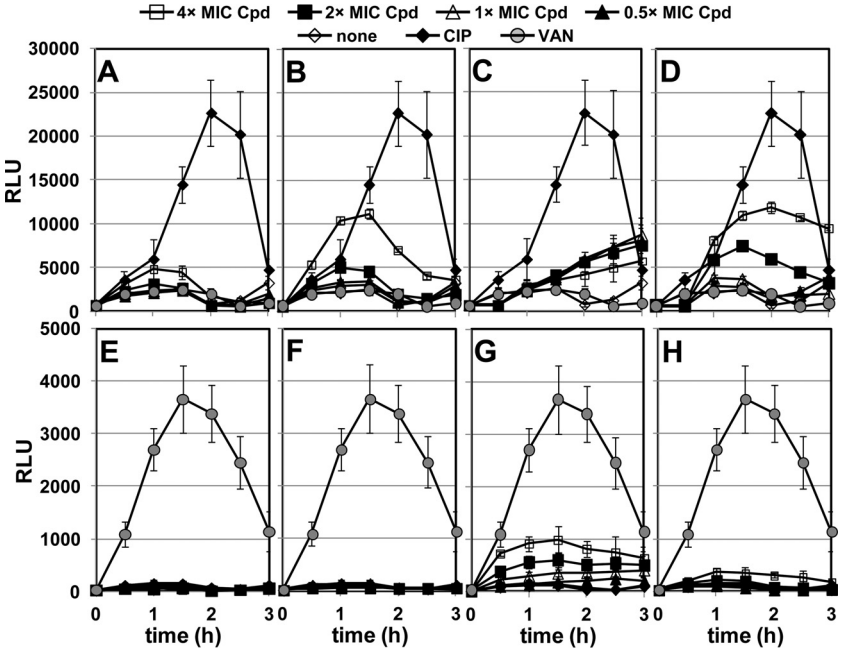

FIG 6 Bis-indoles induce the DNA damage-inducible SOS response, but not the cell wall stress stimulon, in *S. aureus*. (A to D) An *S. aureus* strain carrying an SOS-inducible reporter construct, consisting of the *recA* promoter fused to an operon encoding bacterial luciferase (*luxABCDE*) on pAmi-Rec (17), was treated with various concentrations of MBX-1066 (A), MBX-1162 (B), MBX-1195 (C), or netropsin (D), and the light emission was monitored over time. Concentrations are expressed as multiples of the MIC (see Table 1). Ciprofloxacin (CIP), an inhibitor of DNA replication, and vancomycin (VAN), an inhibitor of cell wall synthesis, were used as positive and negative controls, respectively. (E to H) An *S. aureus* strain carrying a cell wall stress-inducible reporter construct, consisting of the *vraX* promoter fused to an operon encoding bacterial luciferase (*luxABCDE*) carried on pAmi-vraX, was treated with various concentrations of MBX-1066 (E), MBX-1162 (F), MBX-1195 (G), or netropsin (H), and the light emission was monitored over time. Vancomycin (VAN) and ciprofloxacin (CIP) were used as positive and negative controls, respectively. Each point on the graph is the average of eight replicates, and the error bars indicate the standard deviations.

these compounds and actually parallels the relative DNA binding affinities of these compounds (see above). Compounds bound to the minor groove of DNA increase the stability of the double helix, which affects the activity of both DNA and RNA polymerases. The affinity of a compound for the minor groove is directly correlated with increased T_m of dsDNA (higher DNA affinity compounds results in higher T_m), which results in greater inhibition of DNA and RNA synthesis. In addition, minor groove binders change the structure of dsDNA, which could sterically block the binding of proteins involved in DNA replication and transcription. Therefore, it is likely that the DNA binding activity of the bis-indoles is a major component of the mechanism of action of these compounds. The proposed mechanism for the bis-indoles is thus consistent with that of other classes of DNA binding antibacterial agents (37).

While the inhibition of DNA and RNA synthesis constitutes a well-established cellular consequence of treatment with a DNA binding agent, the potent inhibition of the other MMS pathways, particularly cell wall synthesis, suggests that there may be additional mechanisms of action, or that the inhibition of cell wall synthesis is a secondary effect. The most likely mechanism that would affect all MMS pathways is membrane disruption; however, we have shown previously that the bis-indoles do not perturb the transmembrane proton gradient (4). Therefore, additional cellular targets for the action of the bis-indoles, if they indeed exist, have yet to be identified. To determine whether these compounds act directly on the cell wall synthetic pathway, we measured the effect of the bis-indoles and netropsin on a strain of *S. aureus* carrying a reporter construct that produces a bioluminescent signal in response to inhibitors of cell wall synthesis. The reporter construct consists of the promoter of *vraX*, which is induced by inhibitors of cell wall and teichoic acid synthesis and is part of the cell wall stress stimulon [CWSS] (15, 16, 38), that has been fused to a bacterial luciferase operon (*luxABCDE*) carried on plasmid (pAmi-vraX). As shown in Fig. 6E to H, exposure of the cell wall stress reporter strain to MBX-1066 (Fig. 6E), MBX-1162 (Fig. 6F), and netropsin (Fig. 6H) did not result in significant bioluminescence, even when concentrations of the compounds were 4× the MIC, indicating that these compounds do not inhibit cell wall synthesis directly. Therefore, it is likely that these compounds inhibit cell wall biosynthesis in the MMS assay through an unidentified, indirect mechanism. For example, the bis-indoles could inhibit uptake of the radiolabeled cell wall precursor (*N*-acetylglucosamine). In contrast, exposure to MBX-1195 (Fig. 6G) resulted in significant levels of bioluminescence, indicating that the compound inhibits cell wall or teichoic acid synthesis; however, the level of inhibition was significantly lower than that of the positive control VAN. Therefore, MBX-1195 appears to work through a different mechanism of action than the bis-indoles that have higher affinities for DNA. For example, MBX-1195 may induce the cell wall stress stimulon by modifying the properties of the cell membrane without perturbing the transmembrane proton gradient, as is the case with daptomycin (39). Further experiments are required to identify the putative target of MBX-1195 in the cell wall biosynthetic pathway.

Bis-indoles induce the SOS response. The DNA binding activity of the bis-indoles raised the possibility that an interaction between these compounds and DNA might result in induction of

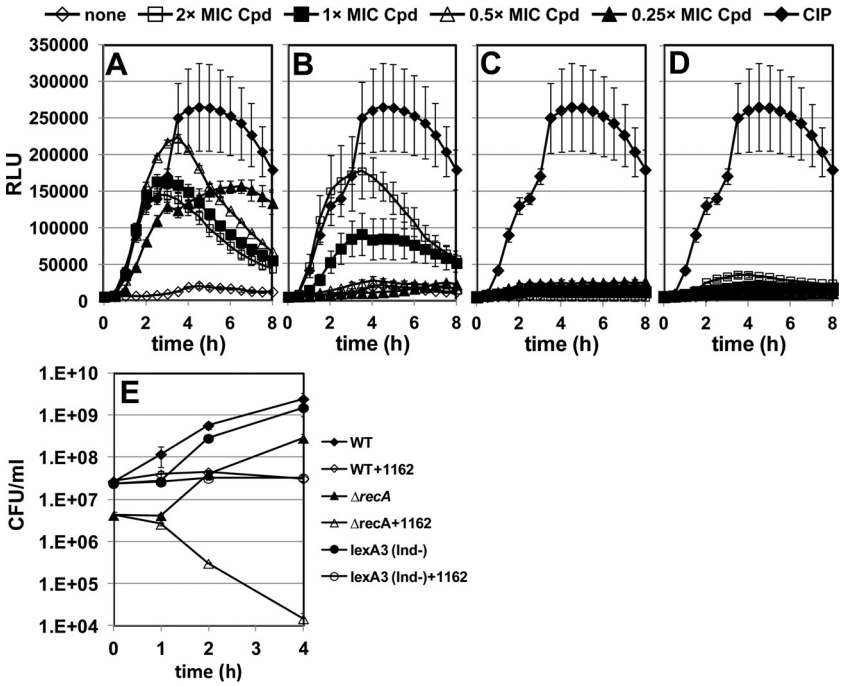

FIG 7 Bis-indoles induce the DNA damage-inducible SOS response in *E. coli*. (A) An *E. coli* strain carrying an SOS-inducible reporter construct consisting of the *sulA* promoter fused to an operon encoding bacterial luciferase (*luxCDABE*) was treated with various concentrations of MBX-1066 (A), MBX-1162 (B), MBX-1195 (C), or netropsin (D), and light emission was monitored over time. Compound concentrations are expressed as multiples of the MIC (see Table 1). Ciprofloxacin (CIP) at a concentration of 0.1 μg/ml (5× the MIC) was used as a positive control. Each point on the graph is the average of eight replicates, and the error bars indicate the standard deviations. (E) A RecA-defective mutant of *E. coli* AB1157 is more sensitive to MBX-1162 (0.016 μg/ml, 0.25× the MIC for WT) than is WT. Each point on the graph is the average of three replicates, and the error bars indicate the standard deviations.

the SOS response, a stress response that is induced by the presence of single-stranded DNA resulting from DNA damage (40), or certain conditions that inhibit DNA replication (41–43). To examine this possibility, we measured the induction of the SOS response in *E. coli* and *S. aureus* cells that were exposed to bis-indoles. Induction of the SOS response was measured using a reporter strains of *E. coli* [GW1000 *glmS*::mini-Tn7 P_{sulA}-*luxCDABE*] and S. aureus [RN4220 pAmi-Rec (17)] that carry reporter constructs consisting of an SOS-inducible promoter fused to the luciferase operon (*luxCDABE*) of *Photorhabdus luminescens*. DNA damage in the reporter strain induces the SOS response, resulting in increased expression of the luciferase operon. Ciprofloxacin (CIP), a fluoroquinolone antibiotic agent that induces the SOS response, was used as a positive control. The results for the *E. coli* reporter strain, shown in Fig. 7A and B, demonstrate that exposure to the higher DNA affinity compounds MBX-1066 (Fig. 7A) and MBX-1162 (Fig. 7B) resulted in induction of the SOS response to levels comparable to positive control, whereas the weakest DNA binding bis-indole, MBX-1195, did not induce the SOS response. In comparison, the lower levels of SOS induction produced at higher concentrations of MBX-1162 are likely due to the rapid bactericidal activity of this compound at concentrations above the MIC (4); this is also likely to be the explanation for the failure of netropsin to induce the SOS response in this assay. The bis-indoles also induced the SOS response in *S. aureus* (Fig. 6A to C); however, the levels of induction were lower than that of the positive control. In addition, MBX-1066 (Fig. 6A) and MBX-1162 (Fig. 6B) induced the SOS response to a lower level than did MBX-1195 (Fig. 6C) and netropsin (Fig. 6D). These data indicate that bis-indoles induce the SOS response in both *E. coli* and *S. aureus*; however, the effects of each compound and the overall level of SOS induction varied between the two organisms. There are several possible explanations for the observed differences. For example, the SOS regulon of *S. aureus* is much more limited than that of *E. coli* (44), which could decrease the range of DNA damage signals to which the SOS regulon of *S. aureus* responds. In addition, the replicative DNA polymerases in *S. aureus* (PolC) and *E. coli* (DnaE) are significantly different in primary amino acid sequence (<20% identity) (45), domain arrangements, the presence of an intrinsic 3′–5′ proofreading exonuclease domain in PolC (but not DnaE), and differential sensitivity to inhibition by nucleotide analogs (46).

If bis-indole exposure results in DNA damage, then SOS-defective mutants should exhibit increased sensitivity to the bis-indole compounds compared to the wild type (WT). Indeed, the MICs for MBX-1066 and MBX-1162 against isogenic Δ*recA* and *lexA3*(Ind−) strains were consistently 2-fold lower than WT (Table 3). In addition, we performed a time-kill assay with *E. coli*

TABLE 3 MICs for bis-indoles against wild-type and SOS-defective strains of *E. coli*

Strain	MIC (μg/ml)		
	MBX-1066	MBX-1162	CIP
Wild type (AB1157)	1	0.5	0.016
Δ*recA* mutant	0.5	0.25	0.002
lexA3 (Ind−) mutant	0.5	0.25	0.004

AB1157 (WT) and Δ*recA* and *lexA3*(Ind−) mutants that were treated with MBX-1162 at a concentration that is minimally bactericidal against the WT (0.016 μg/ml, 0.25× the MIC). As shown in Fig. 7E, a 0.016-μg/ml concentration of MBX-1162 did not decrease the viability of the WT or the *lexA3* (Ind−) strains, but it reduced the viability of the Δ*recA* strain by ≥100-fold over 4 h. These results indicate that the recombination-repair activity and not the SOS-regulatory function of RecA is required for coping with the effects of bis-indoles. The recombination-repair activity of RecA is required for DNA strand break repair (40), suggesting that bis-indole exposure causes DNA strand breaks. While the data presented above do not directly demonstrate the presence of DNA lesions after bis-indole exposure, induction of the SOS response in *E. coli* and *S. aureus* is indicative of DNA damage. Due to the chemical properties of the bis-indoles, it is unlikely that these compounds react with DNA to covalently modify the DNA. However, it is possible that the bis-indoles bound to the DNA minor groove block the progression of the DNA replication machinery and replication is initiated further downstream, resulting in single-stranded DNA. Alternatively, minor groove binding compounds, such as Hoechst 33342, have been shown to inhibit human topoisomerase I and trap the human topoisomerase I cleavage complex (47), which is the basis for the antitumor activity of these compounds. Although only speculation at this point, it is possible that the bis-indoles interfere with the activity of a bacterial topoisomerase I or II enzyme, resulting in single- or double-stranded DNA breaks. Further experiments are needed to determine the exact nature of the DNA damage produced by the bis-indoles.

The preceding studies indicate that the bis-indole series of compounds under investigation here target and bind to double-stranded DNA *in vitro* and within bacterial cells. These agents display a distinct preference for A/T-rich DNA and behave in a fashion quite reminiscent of structurally similar compounds such as DAPI, netropsin, and the clinically used diamidine, pentamidine. Indeed, the bis-indoles described here are very similar to pentamidine and other DNA-targeted diamidine derivatives in that these compounds can enter cells, target and bind to genomic DNA, and lead to the inhibition of DNA and RNA biosynthesis. In further analogy to the bis-indoles described here, diamidines such as pentamidine are also thought to target genomic DNA in conjunction with disruptions of other biological processes (48). Overall, these observations support the notion that the bis-indoles most likely bind to the DNA minor groove as a primary target and in doing so inhibit RNA and DNA biosynthesis. In addition, the bis-indoles induce the SOS response in *E. coli* and *S. aureus*, suggesting that exposure to these compounds results in single-stranded DNA (the SOS inducing signal) through at least two possible mechanisms: (i) the inhibition of DNA polymerase or (ii) the production of DNA damage. In parallel, the bis-indoles most likely inhibit other macromolecular synthetic pathways through an indirect mechanism(s). Because the proposed mechanism of action of antibacterial activity is similar to the mechanism of antifungal activity (7), it is likely that the DNA binding activity of the bis-indoles is responsible for the cytotoxicity of this class of compounds against mammalian cell lines, which precludes their potential use as a systemic or topical therapeutic agent in humans.

ACKNOWLEDGMENTS

We thank Graham Walker (Massachusetts Institute of Technology, Cambridge, MA) for kindly providing the strains GW1000, GW1000 *lexA3*(Ind−), GW1000 Δ*lexA300*::spec(Def), and GW1000 Δ*recA*::kan.

This study was supported by the Defense Threat Reduction Agency of the U.S. Department of Defense under contract HDTRA1-06-C-0042.

The content is solely the responsibility of the authors and does not necessarily represent the official views of the U.S. Department of Defense.

FUNDING INFORMATION

This work, including the efforts of Timothy J. Opperman, John D. Williams, Donald T. Moir, and Terry L. Bowlin, was funded by DOD | Defense Threat Reduction Agency (DTRA) (HDTRA1-06-C-0042).

REFERENCES

1. **Boucher HW, Talbot GH, Benjamin DK, Jr, Bradley J, Guidos RJ, Jones RN, Murray BE, Bonomo RA, Gilbert D.** 2013. 10 × '20 progress—development of new drugs active against gram-negative bacilli: an update from the Infectious Diseases Society of America. Clin Infect Dis **56:**1685–1694. http://dx.doi.org/10.1093/cid/cit152.
2. **Boucher HW, Talbot GH, Bradley JS, Edwards JE, Gilbert D, Rice LB, Scheld M, Spellberg B, Bartlett J.** 2009. Bad bugs, no drugs: no ESKAPE! An update from the Infectious Diseases Society of America. Clin Infect Dis **48:**1–12. http://dx.doi.org/10.1086/595011.
3. **Butler MM, Williams JD, Peet NP, Moir DT, Panchal RG, Bavari S, Shinabarger DL, Bowlin TL.** 2010. Comparative in vitro activity profiles of novel bis-indole antibacterials against gram-positive and gram-negative clinical isolates. Antimicrob Agents Chemother **54:**3974–3977. http://dx.doi.org/10.1128/AAC.00484-10.
4. **Panchal RG, Ulrich RL, Lane D, Butler MM, Houseweart C, Opperman T, Williams JD, Peet NP, Moir DT, Nguyen T, Gussio R, Bowlin T, Bavari S.** 2009. Novel broad-spectrum bis-(imidazolinylindole) derivatives with potent antibacterial activities against antibiotic-resistant strains. Antimicrob Agents Chemother **53:**4283–4291. http://dx.doi.org/10.1128/AAC.01709-08.
5. **Jacobs MR, Bajaksouzian S, Good CE, Butler MM, Williams JD, Peet NP, Bowlin TL, Endimiani A, Bonomo RA.** 2011. Novel bis-indole agents active against multidrug-resistant *Acinetobacter baumannii*. Diagn Microbiol Infect Dis **69:**114–116. http://dx.doi.org/10.1016/j.diagmicrobio.2010.08.014.
6. **Panchal RG, Lane D, Boshoff HI, Butler MM, Moir DT, Bowlin TL, Bavari S.** 2013. Bis-imidazolinylindoles are active against methicillin-resistant *Staphylococcus aureus* and multidrug-resistant *Mycobacterium tuberculosis*. J Antibiot **66:**47–49. http://dx.doi.org/10.1038/ja.2012.93.
7. **Nguyen ST, Kwasny SM, Ding X, Williams JD, Peet NP, Bowlin TL, Opperman TJ.** 2015. Synthesis and antifungal evaluation of head-to-head and head-to-tail bisamidine compounds. Bioorg Med Chem **23:**5789–5798. http://dx.doi.org/10.1016/j.bmc.2015.07.006.
8. **Novick R.** 1967. Properties of a cryptic high-frequency transducing phage in *Staphylococcus aureus*. Virology **33:**155–166. http://dx.doi.org/10.1016/0042-6822(67)90105-5.
9. **Mesak LR, Miao V, Davies J.** 2008. Effects of subinhibitory concentrations of antibiotics on SOS and DNA repair gene expression in *Staphylococcus aureus*. Antimicrob Agents Chemother **52:**3394–3397. http://dx.doi.org/10.1128/AAC.01599-07.
10. **Tegos G, Stermitz FR, Lomovskaya O, Lewis K.** 2002. Multidrug pump inhibitors uncover remarkable activity of plant antimicrobials. Antimicrob Agents Chemother **46:**3133–3141. http://dx.doi.org/10.1128/AAC.46.10.3133-3141.2002.
11. **Bagg A, Kenyon CJ, Walker GC.** 1981. Inducibility of a gene product required for UV and chemical mutagenesis in *Escherichia coli*. Proc Natl Acad Sci U S A **78:**5749–5753. http://dx.doi.org/10.1073/pnas.78.9.5749.
12. **Moir DT, Ming D, Opperman T, Schweizer HP, Bowlin TL.** 2007. A high-throughput, homogeneous, bioluminescent assay for *Pseudomonas aeruginosa* gyrase inhibitors and other DNA-damaging agents. J Biomol Screen **12:**855–864. http://dx.doi.org/10.1177/1087057107304729.
13. **Choi KH, Gaynor JB, White KG, Lopez C, Bosio CM, Karkhoff-Schweizer RR, Schweizer HP.** 2005. A Tn7-based broad-range bacterial cloning and expression system. Nat Methods **2:**443–448. http://dx.doi.org/10.1038/nmeth765.
14. **Dengler V, Meier PS, Heusser R, Berger-Bachi B, McCallum N.** 2011.

Induction kinetics of the *Staphylococcus aureus* cell wall stress stimulon in response to different cell wall active antibiotics. BMC Microbiol **11:**16. http://dx.doi.org/10.1186/1471-2180-11-16.

15. **McAleese F, Wu SW, Sieradzki K, Dunman P, Murphy E, Projan S, Tomasz A.** 2006. Overexpression of genes of the cell wall stimulon in clinical isolates of *Staphylococcus aureus* exhibiting vancomycin-intermediate *S. aureus*-type resistance to vancomycin. J Bacteriol **188:** 1120–1133. http://dx.doi.org/10.1128/JB.188.3.1120-1133.2006.
16. **Utaida S, Dunman PM, Macapagal D, Murphy E, Projan SJ, Singh VK, Jayaswal RK, Wilkinson BJ.** 2003. Genome-wide transcriptional profiling of the response of *Staphylococcus aureus* to cell-wall-active antibiotics reveals a cell-wall-stress stimulon. Microbiology **149:**2719–2732. http://dx.doi.org/10.1099/mic.0.26426-0.
17. **Mesak LR, Yim G, Davies J.** 2009. Improved lux reporters for use in *Staphylococcus aureus*. Plasmid **61:**182–187. http://dx.doi.org/10.1016/j.plasmid.2009.01.003.
18. **Schmitz FJ, Fluit AC, Luckefahr M, Engler B, Hofmann B, Verhoef J, Heinz HP, Hadding U, Jones ME.** 1998. The effect of reserpine, an inhibitor of multidrug efflux pumps, on the in-vitro activities of ciprofloxacin, sparfloxacin and moxifloxacin against clinical isolates of *Staphylococcus aureus*. J Antimicrob Chemother **42:**807–810. http://dx.doi.org/10.1093/jac/42.6.807.
19. **Williams JD, Nguyen ST, Gu S, Ding X, Butler MM, Tashjian TF, Opperman TJ, Panchal RG, Bavari S, Peet NP, Moir DT, Bowlin TL.** 2013. Potent and broad-spectrum antibacterial activity of indole-based bisamidine antibiotics: Synthesis and SAR of novel analogs of MBX 1066 and MBX 1090. Bioorg Med Chem **21:**7790–7806. http://dx.doi.org/10.1016/j.bmc.2013.10.014.
20. **Beuria TK, Santra MK, Panda D.** 2005. Sanguinarine blocks cytokinesis in bacteria by inhibiting FtsZ assembly and bundling. Biochemistry **44:** 16584–16593. http://dx.doi.org/10.1021/bi050767+.
21. **Boger DL, Fink BE, Brunette SR, Tse WC, Hedrick MP.** 2001. A simple, high-resolution method for establishing DNA binding affinity and sequence selectivity. J Am Chem Soc **123:**5878–5891. http://dx.doi.org/10.1021/ja010041a.
22. **Boger DL, Tse WC.** 2001. Thiazole orange as the fluorescent intercalator in a high-resolution fid assay for determining DNA binding affinity and sequence selectivity of small molecules. Bioorg Med Chem **9:**2511–2518. http://dx.doi.org/10.1016/S0968-0896(01)00243-7.
23. **Lewis MA, Long EC.** 2006. Fluorescent intercalator displacement analyses of DNA binding by the peptide-derived natural products netropsin, actinomycin, and bleomycin. Bioorg Med Chem **14:**3481–3490. http://dx.doi.org/10.1016/j.bmc.2006.01.006.
24. **Tanious FA, Laine W, Peixoto P, Bailly C, Goodwin KD, Lewis MA, Long EC, Georgiadis MM, Tidwell RR, Wilson WD.** 2007. Unusually strong binding to the DNA minor groove by a highly twisted benzimidazole diphenylether: induced fit and bound water. Biochemistry **46:**6944–6956. http://dx.doi.org/10.1021/bi700288g.
25. **Tse WC, Boger DL.** 2004. A fluorescent intercalator displacement assay for establishing DNA binding selectivity and affinity. Accounts Chem Res **37:**61–69. http://dx.doi.org/10.1021/ar030113y.
26. **Cotsonas-King A, Wu L.** 2009. Macromolecular synthesis and membrane perturbation assays for mechanisms of action studies of antimicrobial agents. Curr Protoc Pharmacol Chapter 13:Unit 13A.7. http://dx.doi.org/10.1002/0471141755.ph13a07s47.
27. **Clinical and Laboratory Standards Institute.** 2006. Methods for dilution antimicrobial susceptibility tests for bacteria that grow aerobically; approved standard, 7th ed, vol M7-A7 26:2. Clinical and Laboratory Standards Institute, Wayne, PA.
28. **Pillai SK, Moellering RC, Eliopoulos GM.** 2005. Antimicrobial combinations, p 365–440. *In* Lorian V (ed), Antibiotics in laboratory medicine, 5th ed. Lippincott/Williams & Wilkins, Philadelphia, PA.
29. **Butler MM, Lamarr WA, Foster KA, Barnes MH, Skow DJ, Lyden PT, Kustigian LM, Zhi C, Brown NC, Wright GE, Bowlin TL.** 2007. Antibacterial activity and mechanism of action of a novel anilinouracil-fluoroquinolone hybrid compound. Antimicrob Agents Chemother **51:** 119–127. http://dx.doi.org/10.1128/AAC.01311-05.
30. **Neidle S.** 2001. DNA minor-groove recognition by small molecules. Natural Prod Rep **18:**291–309. http://dx.doi.org/10.1039/a705982e.
31. **Wei D, Wilson WD, Neidle S.** 2013. Small-molecule binding to the DNA minor groove is mediated by a conserved water cluster. J Am Chem Soc **135:**1369–1377. http://dx.doi.org/10.1021/ja308952y.
32. **Chai Y, Munde M, Kumar A, Mickelson L, Lin S, Campbell NH, Banerjee M, Akay S, Liu Z, Farahat AA, Nhili R, Depauw S, David-Cordonnier MH, Neidle S, Wilson WD, Boykin DW.** 2014. Structure-dependent binding of arylimidamides to the DNA minor groove. Chembiochem **15:**68–79. http://dx.doi.org/10.1002/cbic.201300622.
33. **Farahat AA, Paliakov E, Kumar A, Barghash AE, Goda FE, Eisa HM, Wenzler T, Brun R, Liu Y, Wilson WD, Boykin DW.** 2011. Exploration of larger central ring linkers in furamidine analogues: synthesis and evaluation of their DNA binding, antiparasitic and fluorescence properties. Bioorg Med Chem **19:**2156–2167. http://dx.doi.org/10.1016/j.bmc.2011.02.045.
34. **Ismail MA, Batista-Parra A, Miao Y, Wilson WD, Wenzler T, Brun R, Boykin DW.** 2005. Dicationic near-linear biphenyl benzimidazole derivatives as DNA-targeted antiprotozoal agents. Bioorg Med Chem **13:**6718–6726. http://dx.doi.org/10.1016/j.bmc.2005.07.024.
35. **Zimmer C, Wahnert U.** 1986. Nonintercalating DNA-binding ligands: specificity of the interaction and their use as tools in biophysical, biochemical and biological investigations of the genetic material. Prog Biophys Mol Biol **47:**31–112. http://dx.doi.org/10.1016/0079-6107(86)90005-2.
36. **Ge Y, Difuntorum S, Touami S, Critchley I, Burli R, Jiang V, Drazan K, Moser H.** 2002. *In vitro* antimicrobial activity of GSQ1530, a new heteroaromatic polycyclic compound. Antimicrob Agents Chemother **46:** 3168–3174. http://dx.doi.org/10.1128/AAC.46.10.3168-3174.2002.
37. **Kaizerman JA, Gross MI, Ge Y, White S, Hu W, Duan JX, Baird EE, Johnson KW, Tanaka RD, Moser HE, Burli RW.** 2003. DNA binding ligands targeting drug-resistant bacteria: structure, activity, and pharmacology. J Med Chem **46:**3914–3929. http://dx.doi.org/10.1021/jm030097a.
38. **Campbell J, Singh AK, Swoboda JG, Gilmore MS, Wilkinson BJ, Walker S.** 2012. An antibiotic that inhibits a late step in wall teichoic acid biosynthesis induces the cell wall stress stimulon in *Staphylococcus aureus*. Antimicrob Agents Chemother **56:**1810–1820. http://dx.doi.org/10.1128/AAC.05938-11.
39. **Muthaiyan A, Silverman JA, Jayaswal RK, Wilkinson BJ.** 2008. Transcriptional profiling reveals that daptomycin induces the *Staphylococcus aureus* cell wall stress stimulon and genes responsive to membrane depolarization. Antimicrob Agents Chemother **52:**980–990. http://dx.doi.org/10.1128/AAC.01121-07.
40. **Friedberg EC, Walker GC, Siede W, Wood RD, Schultz RA, Ellenberger T.** 2006. DNA repair and mutagenesis, 2nd ed. ASM Press, Washington, DC.
41. **Barbe J, Villaverde A, Guerrero R.** 1987. Induction of the SOS response by hydroxyurea in *Escherichia coli* K12. Mutat Res **192:**105–108. http://dx.doi.org/10.1016/0165-7992(87)90105-9.
42. **Lewin CS, Amyes SG.** 1991. The role of the SOS response in bacteria exposed to zidovudine or trimethoprim. J Med Microbiol **34:**329–332. http://dx.doi.org/10.1099/00222615-34-6-329.
43. **Rosado H, Rahman KM, Feuerbaum EA, Hinds J, Thurston DE, Taylor PW.** 2011. The minor groove-binding agent ELB-21 forms multiple interstrand and intrastrand covalent cross-links with duplex DNA and displays potent bactericidal activity against methicillin-resistant *Staphylococcus aureus*. J Antimicrob Chemother **66:**985–996. http://dx.doi.org/10.1093/jac/dkr044.
44. **Cirz RT, Jones MB, Gingles NA, Minogue TD, Jarrahi B, Peterson SN, Romesberg FE.** 2007. Complete and SOS-mediated response of *Staphylococcus aureus* to the antibiotic ciprofloxacin. J Bacteriol **189:**531–539. http://dx.doi.org/10.1128/JB.01464-06.
45. **Pacitti DF, Barnes MH, Li DH, Brown NC.** 1995. Characterization and overexpression of the gene encoding *Staphylococcus aureus* DNA polymerase III. Gene **165:**51–56. http://dx.doi.org/10.1016/0378-1119(95)00377-I.
46. **Wright GE, Brown NC, Xu WC, Long ZY, Zhi C, Gambino JJ, Barnes MH, Butler MM.** 2005. Active site directed inhibitors of replication-specific bacterial DNA polymerases. Bioorg Med Chem Lett **15:**729–732. http://dx.doi.org/10.1016/j.bmcl.2004.11.016.
47. **Chen AY, Yu C, Gatto B, Liu LF.** 1993. DNA minor groove-binding ligands: a different class of mammalian DNA topoisomerase I inhibitors. Proc Natl Acad Sci U S A **90:**8131–8135. http://dx.doi.org/10.1073/pnas.90.17.8131.
48. **Soeiro MN, Werbovetz K, Boykin DW, Wilson WD, Wang MZ, Hemphill A.** 2013. Novel amidines and analogues as promising agents against intracellular parasites: a systematic review. Parasitology **140:**929–951. http://dx.doi.org/10.1017/S0031182013000292.